

The First Examples of Isonitrile Insertion into a Phosphido Bridge and the Crystal and Molecular Structures of $[\text{Pt}_2(\mu\text{-P}(\text{Bu}^t)_2)\{\mu, \eta^2\text{-P}(\text{Bu}^t)_2\text{C}(\text{=NAr})\}(\text{CNAr})_2]$ and $[\text{Pt}\{\mu, \eta^2\text{-P}(\text{Bu}^t)_2\text{C}(\text{NHAr})\}(\text{CNAr})]_2(\text{CF}_3\text{SO}_3)_2$ (Ar = *p*-Tolyl)

Serena Cristofani,[†] Piero Leoni,^{*,†} Marco Pasquali,[†] Frank Eisentraeger,^{‡,§} and Alberto Albinati[‡]

Dipartimento di Chimica e Chimica Industriale, Università di Pisa, I-56126 Pisa, Italy, and Istituto di Chimica Farmaceutica, Viale Abruzzi 42, I-20131 Milano, Italy

Received June 1, 2000

The platinum(I) dinuclear carbonyl $[\text{Pt}_2(\mu\text{-P}(\text{Bu}^t)_2)_2(\text{P}(\text{Bu}^t)_2\text{H})(\text{CO})]$ (**1**) reacts with organic isonitriles RNC (R = *p*-tolyl, Bu^t, PhCH₂), yielding the mono- and disubstituted derivatives $[\text{Pt}_2(\mu\text{-P}(\text{Bu}^t)_2)_2(\text{P}(\text{Bu}^t)_2\text{H})(\text{CNR})]$ (**2**, R = *p*-tolyl; **3**, R = Bu^t; **4**, R = PhCH₂) and $[\text{Pt}(\mu\text{-P}(\text{Bu}^t)_2)(\text{CNR})]_2$ (**5**, R = *p*-tolyl; **6**, R = Bu^t; **7**, R = PhCH₂). Only with the aromatic isonitrile does the reaction proceed through two further well-separated steps, giving $[\text{Pt}_2(\mu\text{-P}(\text{Bu}^t)_2)\{\mu, \eta^2\text{-P}(\text{Bu}^t)_2\text{C}(\text{=NAr})\}(\text{CNAr})_2]$ (**8**) and $[\text{Pt}\{\mu, \eta^2\text{-P}(\text{Bu}^t)_2\text{C}(\text{=NAr})\}(\text{CNAr})]_2$ (**9**). These arise from the unprecedented reversible isonitrile insertion into the M–P bonds of the phosphido-bridges. When **8** or **9** are reacted with CF₃SO₃H, the cyclic carbenes $[\text{Pt}_2(\mu\text{-P}(\text{Bu}^t)_2)\{\mu, \eta^2\text{-P}(\text{Bu}^t)_2\text{C}(\text{NHAr})\}(\text{CNAr})_2]\text{CF}_3\text{SO}_3$ (**10**) and $[\text{Pt}\{\mu, \eta^2\text{-P}(\text{Bu}^t)_2\text{C}(\text{NHAr})\}(\text{CNAr})]_2(\text{CF}_3\text{SO}_3)_2$ (**11**) are respectively formed. The crystal and molecular structures of complexes **8** and **11** were solved by X-ray diffraction.

Introduction

Isonitrile ligands insert easily into various types of metal–carbon bonds, yielding iminoacyl derivatives of great interest in organometallic synthesis.¹ Even though these reactions are quite common, related insertions into other metal–element bonds are by far less studied. Some examples of insertion into M–H,² M–O,³ or M–N⁴ bonds have been reported, but few cases are known with the heavier main-group elements.

For example, only recently have the first insertions into metal–sulfur or –selenium bonds been discussed^{5a,b} (examples of isonitrile insertion into Os–S bonds were also suggested in previous reports),^{5c,d} and the insertion into M–X (Cl, Br) bonds has been first suggested^{6a–d}

and then denied.^{6e} Moreover, palladium-catalyzed isonitrile insertions into Si–Si bonds were thought to proceed via the insertion into Pd–Si bonds.⁷

As far as the metal–phosphorus bonds are concerned, we are only aware of a few recent data on the insertion into the M–P bonds of a *terminal* phosphide bonded to zirconium⁸ or uranium⁹ or of a phosphazirconacyclobutene.¹⁰ The related insertion of carbon monoxide is also very rare, and the insertion into the M–P bonds of Cp*HfCl₂(PBU^t)₂, reported by Bercaw et al.,¹¹ is still the unique example (if one neglects the insertion of CO and other ligands into the M–P bonds of phosphido-bridged derivatives).¹²

[†] Università di Pisa.

[‡] Istituto di Chimica Farmaceutica.

[§] Permanent address: Organisch-Chemisches Institut, Universität Heidelberg, Heidelberg, Germany.

(1) Singleton, E.; Oosthuizen, H. E. *Adv. Organomet. Chem.* **1983**, *22*, 209.

(2) (a) Tanase, T.; Ohizumi, T.; Kobayashi, K.; Yamamoto, Y. *Organometallics* **1996**, *15*, 3404. (b) Christian, D. F.; Clark, H. C.; Stepaniak, R. F. *J. Organomet. Chem.* **1976**, *112*, 209. (c) Hogarth, G.; Lavender, M. H.; Shukri, K. *Organometallics* **1995**, *14*, 2325. (d) Clark, J. R.; Fanwick, P. E.; Rothwell, I. P. *Organometallics* **1996**, *15*, 3232. (e) Wolczanski, P. T.; Bercaw, J. E. *J. Am. Chem. Soc.* **1979**, *101*, 6450.

(3) Michelin, R. A.; Ros, R. *J. Organomet. Chem.* **1979**, *169*, C42.

(4) (a) Galakhov, M.; Gomez-Sal, P.; Martin, A.; Mena, M.; Yelamos, C. *Eur. J. Inorg. Chem.* **1998**, 1319. (b) Kim, Y. J.; Kim, D. H.; Lee, J. Y.; Lee, S. W. *J. Organomet. Chem.* **1997**, *538*, 189. (c) Beck, W.; Burger, K.; Felhammer, W. P. *Chem. Ber.* **1971**, *104*, 1816. (d) Chisholm, M. H.; Hammond, C. E.; Ho, D.; Huffman, J. C. *J. Am. Chem. Soc.* **1986**, *108*, 7860. (e) Dormond, A.; Aaliti, A.; Moise, C. *J. Chem. Soc., Chem. Commun.* **1985**, 1231. (f) Glueck, D. S.; Hollander, F. J.; Bergman, R. G. *J. Am. Chem. Soc.* **1989**, *111*, 2719. (g) Zanella, P.; Brianese, N.; Casellato, U.; Ossola, F.; Porchia, M.; Rossetto, G.; Graziani, R. *J. Chem. Soc., Dalton Trans.* **1987**, 2039.

(5) (a) Kuniyasu, H.; Sugoh, K.; Su, M. S.; Kurosawa, H. *J. Am. Chem. Soc.* **1997**, *119*, 4669. (b) Kuniyasu, H.; Maruyama, A.; Kurosawa, H. *Organometallics* **1998**, *17*, 908. (c) Grundy, K. R.; Roper, W. R. *J. Organomet. Chem.* **1976**, *113*, C45. (d) Clark, G. R.; Collins, T. J.; Hall, D.; James, S. M.; Roper, W. R. *J. Organomet. Chem.* **1977**, *141*, C5.

(6) (a) Behnam-Dahkordy, M.; Crociani, B.; Nicolini, M.; Richards, R. L. *J. Organomet. Chem.* **1979**, *181*, 69. (b) Crociani, B.; Nicolini, M.; Richards, R. L. *J. Organomet. Chem.* **1975**, *101*, C1. (c) Crociani, B.; Richards, R. L. *J. Chem. Soc., Chem. Commun.* **1973**, 127. (d) Behnam-Dahkordy, M.; Crociani, B.; Richards, R. L. *J. Chem. Soc., Dalton Trans.* **1977**, 2015. (e) Silverman, L. D.; Dewan, J. C.; Giandomenico, C. M.; Lippard, S. J. *Inorg. Chem.* **1980**, *19*, 3379.

(7) Ito, Y.; Sugimoto, M.; Matsuura, T.; Murakami, M. *J. Am. Chem. Soc.* **1991**, *113*, 8899.

(8) Lindenberg, F.; Sieler, J.; Hey-Hawkins, E. *Polyhedron* **1996**, *15*, 1459.

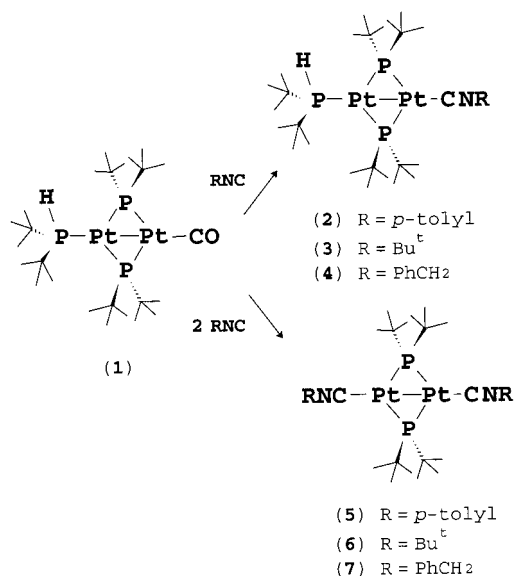
(9) Zanella, P.; Brianese, N.; Casellato, U.; Ossola, F.; Porchia, M.; Rossetto, G.; Graziani, R. *J. Chem. Soc., Dalton Trans.* **1987**, 2039.

(10) Breen, T. L.; Stephan, D. W. *Organometallics* **1996**, *15*, 5729.

(11) Roddick, D. M.; Santarsiero, B. D.; Bercaw, J. E. *J. Am. Chem. Soc.* **1985**, *107*, 4670.

(12) Regragui, R.; Dixneuf, P. H.; Taylor, N. J.; Carty, A. J. *Organometallics* **1984**, *3*, 814.

Scheme 1



To the best of our knowledge, the insertion of isonitriles into a bridging phosphide is yet unreported.

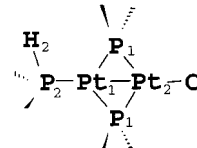
Results and Discussion

Substitution Reactions. Orange-yellow toluene solutions of $[\text{Pt}_2(\mu\text{-P}^t\text{Bu}_2)_2(\text{P}^t\text{Bu}_2\text{H})(\text{CO})]$ (**1**)¹³ were reacted with equimolar amounts of organic isonitriles (RNC, R = *p*-tolyl, Bu^t, PhCH₂), yielding deep orange solutions of the corresponding monosubstituted derivatives $[\text{Pt}_2(\mu\text{-P}^t\text{Bu}_2)_2(\text{P}^t\text{Bu}_2\text{H})(\text{CNR})]$ (**2**, R = *p*-tolyl; **3**, R = Bu^t; **4**, R = PhCH₂) (Scheme 1). The new complexes were formed in nearly quantitative yields (as observed by NMR; much faster reactions occur with the aromatic ligand (see the Experimental Section)) and were isolated as orange solids and characterized by elemental analyses and IR and multinuclear NMR spectroscopy (Table 1).

As can be seen by comparing the data of Table 1, ³¹P and ¹⁹⁵Pt NMR spectra are very similar to the corresponding spectra of complex **1**, which have been thoroughly discussed in a previous paper,¹³ where the crystal and molecular structure of **1** was also reported. Therefore, the spectral features will not be further discussed.

The very low ν_{CN} frequencies in the IR spectra of **2** and **3** deserve a brief comment. First of all they show, together with the low value of ν_{CO} found in complex **1**, that the Pt₂(μ-PBu₂)₂ core has a substantial π basicity, enhanced by the good σ-donor properties of the PBu₂H ligand. Moreover, it should be noted that most of the known values of ν_{CN} for terminally bonded isonitriles fall above 2000 cm⁻¹; however, it should be kept in mind that, although a great number of isonitrile complexes are known, very few are directly comparable to complexes **2–4**. For a meaningful comparison (1) the complex should bear only one isonitrile ligand, together with other good σ-donor ligands, and the metal(s) should be in a relatively low oxidation state and (2) it should not bear other good π-acceptor ligands or a positive

Table 1. Significant NMR (δ (ppm), *J* (Hz)) and IR (cm⁻¹) Parameters for Complexes **1–4**



	1 ^a	2	3	4
δ _{P1}	295.8	295.0	288.6	289.3
δ _{P2}	60.7	62.7	61.2	61.2
δ _{Pt1}	-5483	-5549	-5586	-5573
δ _{Pt2}	-5220	-5162	-5252	-5249
δ _{H2}	6.2	6.3	6.3	6.3
² J _{P1P2}	38	41	41	41
¹ J _{P1Pt1}	2623	2665	2647	2642
¹ J _{P1Pt2}	2431	2402	2543	2533
² J _{P2Pt2}	31	46	41	38
¹ J _{P2Pt1}	4660	4695	4724	4716
¹ J _{P2H2}	328	324	321	318
³ J _{P1H2}	14	15	18	17
² J _{Pt1H2}	27	17	18	18
¹ J _{Pt1Pt2}	185	178	127	188
ν _{PH}	2277	2264	2259	2256
ν _{CN} ^b	1956(ν _{CO})	1936	1975	2029

^a From ref 13. ^b ν_{CN} of the free ligands 2125 (*p*-tolyl-NC), 2134 (Bu^tNC), and 2146 cm⁻¹ (PhCH₂NC).

charge. A limited number of complexes satisfy all (or nearly all) these conditions; for example, the neutral M(0) derivatives Fe(PMe₃)₂(CNR)₃,¹⁴ M(CNR)₂(dppe)₂ (M = Mo, W),¹⁵ *trans*-[Mo(PhNC)₂(Me₈[16]aneS₄)],¹⁶ and Mo(η⁶-PhPMePh)(CNCMe₃)(PMePh₂)₂¹⁷ all exhibit ν_{CN} values below 2000 cm⁻¹.

When the molar ratio RNC/**1** was increased, complex **1** was cleanly converted into the corresponding bis(isonitrile) derivatives [Pt(μ-PBu₂)(CNR)]₂ (**5**, R = *p*-tolyl; **6**, R = Bu^t; **7**, R = PhCH₂); the reactions are nearly quantitative (³¹P NMR), and complexes **5–7** were isolated as analytically pure red-orange powders in satisfactory yields (48–72%). The ³¹P{¹H} NMR spectra exhibit the expected pattern (a singlet with ¹⁹⁵Pt satellites, comprising a 1:8:18:8:1 quintet with *J*_{app} = ¹J_{PPt}/2)¹⁸ at low fields (297.7 ppm, ¹J_{PPt} = 2557 Hz for **5**; 293.1 ppm, ¹J_{PPt} = 2632 Hz for **6**; 294.7 ppm, ¹J_{PPt} = 2649 Hz for **7**) for the equivalent P-bridging nuclei, and the ¹⁹⁵Pt{¹H} NMR spectra give a unique signal for the equivalent Pt nuclei (triplets (¹J_{PPt} as above) at -5177, -5264, and -5268 ppm, respectively). ¹H and ¹³C{¹H} NMR spectra (see Experimental Section) were consistent with structures **5–7**, and the stretching vibrations of the CN groups give strong and broad IR absorptions at 2063, 2033 (**5**), 2175, 2167 (**6**), and 2073 (**7**) cm⁻¹. Reasonably, the increase of ν_{CN}, compared to that observed in **2–4**, is due to the substitution of a phos-

(14) Jones, W. D.; Foster, G. P.; Putinas, J. M. *Inorg. Chem.* **1987**, *26*, 2120.

(15) Chatt, J.; Elson, C. M.; Pombeiro, A. J. L.; Richards, R. L.; Royston, G. H. D. *J. Chem. Soc., Dalton Trans.* **1978**, 165.

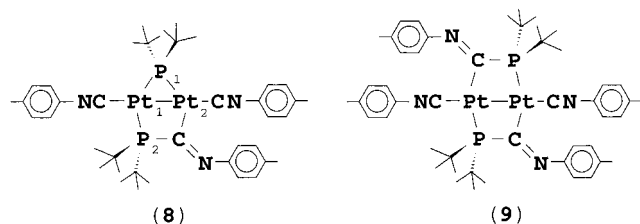
(16) Adachi, T.; Sasaki, N.; Ueda, T.; Kaminaka, M.; Yoshida, T. *J. Chem. Soc., Chem. Commun.* **1989**, 1320.

(17) Luck, R. L.; Morris, R. H.; Sawyer, J. F. *Organometallics* **1984**, *3*, 247.

(18) (a) Hill, G. S.; Puddephatt, R. J. *J. Am. Chem. Soc.* **1996**, *118*, 8745. (b) Mole, L.; Spencer, J. L.; Litster, S. A.; Redhouse, A. D.; Carr, N.; Orpen, A. G. *J. Chem. Soc., Dalton Trans.* **1996**, 2315. (c) Knobler, C. B.; Kaesz, H. D.; Minghetti, G.; Bandini, A. L.; Banditelli, G.; Bonati, F. *Inorg. Chem.* **1983**, *22*, 2324. (d) Tulip, T. H.; Yamagata, T.; Yoshida, T.; Wilson, R. D.; Ibers, J. A.; Otsuka, S. *Inorg. Chem.* **1979**, *18*, 2239.

(13) Leoni, P.; Chiaradonna, G.; Pasquali, M.; Marchetti, F. *Inorg. Chem.* **1999**, *38*, 253.

Chart 1



phine with a less σ -basic isonitrile and to the sharing of π -donation on two RNC ligands in **5**–**7**.

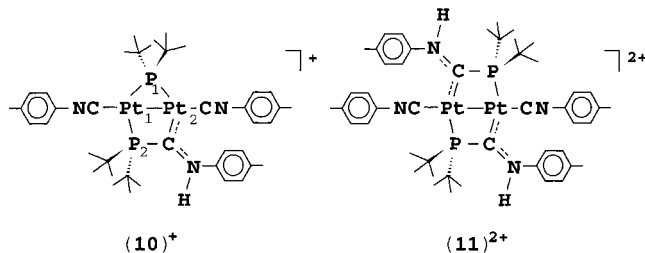
Insertion Reactions. While complexes **6** and **7** remain unchanged in the presence of a large excess of the corresponding isonitrile ligand, complex **5** reacts further. After the addition of 3.5 equiv of *p*-tolylisonitrile, a toluene solution of complex **1** soon becomes (1 h) deep red and contains only $[\text{Pt}_2(\mu\text{-P}(\text{Bu}^t)_2)\{\mu, \eta^2\text{-P}(\text{Bu}^t)_2\text{C}(\text{=NAr})\}(\text{CNAr})_2]$ (**8**) (Chart 1), arising from the insertion of an isonitrile molecule into one of the Pt–P(μ) bonds.

The structure of complex **8** was assigned on the basis of its spectroscopic features and confirmed by an X-ray crystallographic study (see below).

Two signals were observed in the $^{31}\text{P}\{^1\text{H}\}$ NMR spectrum: one was still found in a region typical for bridging phosphides spanning a metal–metal bond¹⁹ (197.0 ppm, P_1), while the other was remarkably high-field-shifted (−37.5 ppm, P_2). Both appear as a central doublet ($^2J_{\text{PP}} = 204$ Hz) flanked by ^{195}Pt satellites, yielding the values of $^1J_{\text{PtPt}_1} = 2820$ Hz, $^1J_{\text{PtPt}_2} = 2351$ Hz, $^1J_{\text{P}_2\text{Pt}_1} = 2280$ Hz, and $^2J_{\text{P}_2\text{Pt}_2} = 257$ Hz (assignment facilitated by comparison with the $^{195}\text{Pt}\{^1\text{H}\}$ NMR spectrum). This exhibits two doublets of doublets (J_{PPt} as above) at −4928.5 and −4523.3 ppm (with satellites yielding the value of $^1J_{\text{PtPt}} = 293$ Hz), which were respectively assigned to Pt_1 and Pt_2 . ^1H and $^{13}\text{C}\{^1\text{H}\}$ NMR spectra (see Experimental Section) were consistent with structure **8**. The stretching vibrations of the CN groups give strong and broad absorptions at 2073, 2040 cm^{-1} and a less intense absorption at 1537 cm^{-1} , which can be assigned to the stretching of the phosphaiminoacyl C=N bond. Complex **8** is stable in the solid state, but in solution, without an excess of *p*-tolyl isocyanide, slowly deinserts the isonitrile molecule, yielding **5**.

When the excess of *p*-tolyl isocyanide is increased further ($\text{ArNC}:\mathbf{1} \geq 5$), a second molecule of the ligand is inserted into a Pt–P(μ) bond of the remaining phosphide, yielding $[\text{Pt}\{\mu, \eta^2\text{-P}(\text{Bu}^t)_2\text{C}(\text{=NAr})\}(\text{CNAr})_2]$ (**9**) (Chart 1), a complex with a centrosymmetric $[\text{PtPC}]_2$ core. Accordingly, a single signal was observed in the $^{195}\text{Pt}\{^1\text{H}\}$ (−4364.3 ppm) and in the $^{31}\text{P}\{^1\text{H}\}$ (−15.1 ppm) NMR spectra (C_6D_6 , 293 K). The latter appears as a central singlet for the equivalent P nuclei. Since these nuclei lose their magnetic equivalence in the two isotopomers containing one ^{195}Pt nucleus, the corresponding satellites (eight lines with intensity ratio 1:2:1:2:2:1:2:1) cannot be interpreted in terms of first-order spectra, but were adequately simulated by using the following values: $^1J_{\text{PPt}} = 1455$ Hz, $^2J_{\text{PPt}} = -265$ Hz, $^3J_{\text{PPt}}$

Chart 2



= 215 Hz, and $^1J_{\text{PtPt}} = 2100$ Hz. This set of coupling constants also reproduces nicely the weak lines due to the isotopomer containing two ^{195}Pt nuclei, as well as the $^{195}\text{Pt}\{^1\text{H}\}$ spectrum (experimental and calculated spectra are provided in the Supporting Information).

^1H and $^{13}\text{C}\{^1\text{H}\}$ NMR spectra (see Experimental Section) were consistent with structure **9**, and the stretching vibrations of the CN groups give a strong and broad IR absorption at 2107 cm^{-1} and a less intense absorption at 1542 cm^{-1} , which can be assigned to the stretching of the phosphaiminoacyl C=N bonds.

As was the case for complex **8**, although more slowly, complex **9** deinserts the isonitrile molecules if dissolved in solution without an excess of *p*-tolyl isocyanide, to give complex **5** quantitatively.

Protonation Reactions. Iminoacyl derivatives formed by isonitrile insertion into M–C bonds can be protonated or alkylated at nitrogen to give Fischer carbenes.²⁰

The same holds true for the new phosphaiminoacyls **8** and **9**. By addition of an equimolar amount of $\text{CF}_3\text{SO}_3\text{H}$ at room temperature, a red solution of complex **8** turned immediately brown and was shown (^{31}P NMR) to contain a unique new product. This was isolated as a red microcrystalline solid in 55% yield and identified as $[\text{Pt}_2(\mu\text{-P}(\text{Bu}^t)_2)\{\mu, \eta^2\text{-P}(\text{Bu}^t)_2\text{C}(\text{NHAr})\}(\text{CNAr})_2]\text{CF}_3\text{SO}_3$ (**10**) (Chart 2). Two doublets ($^2J_{\text{PP}} = 215$ Hz) were observed in the $^{31}\text{P}\{^1\text{H}\}$ NMR spectrum (CDCl_3 , 293 K) at 208.4 (P_1) and 27.0 ppm (P_2), both flanked by ^{195}Pt satellites ($^1J_{\text{PtPt}_1} = 3062$, 2632 Hz, $^1J_{\text{PtPt}_2} = 2380$ Hz, $^2J_{\text{P}_2\text{Pt}_1} = 216$ Hz; note the large downfield shift of P_2 ($\Delta\delta = 64.5$ ppm) compared to the corresponding phosphorus in **8**). The $^{13}\text{C}\{^1\text{H}\}$ and ^1H NMR spectra (see Experimental Section) were consistent with the structure given for **10**. The latter shows for the NH proton a broad resonance at 14.3 ppm with satellites ($^3J_{\text{HPt}} = 120$ Hz); this large coupling constant implies a trans disposition of the nuclei.²¹

The $^{195}\text{Pt}\{^1\text{H}\}$ NMR spectrum (CDCl_3 , 293 K) consists of two doublets of doublets at −5085 ($^1J_{\text{PtP}} = 2380$, 3062 Hz; Pt_1) and −4420 ($^1J_{\text{PtP}} = 2632$ Hz, $^2J_{\text{PtP}} = 216$ Hz; Pt_2) ppm. The latter is further split in the proton-coupled spectrum by the coupling to the NH proton.

The di-inserted derivative **9** reacts analogously with 2 equiv of $\text{CF}_3\text{SO}_3\text{H}$, yielding the bis(carbene) $[\text{Pt}\{\mu, \eta^2\text{-P}(\text{Bu}^t)_2\text{C}(\text{NHAr})\}(\text{CNAr})_2](\text{CF}_3\text{SO}_3)_2$ (**11**). The NMR parameters (see Experimental Section) compare well with the corresponding parameters of complex **10** and will not be discussed further. The structure of **11** has been confirmed by an X-ray crystallographic study (see below).

(19) (a) Garrou, P. E. *Chem. Rev.* **1981**, *81*, 229. (b) Carty, A. J.; MacLaughlin, S. A.; Nucciarone, D. In *^{31}P NMR Spectroscopy in Stereochemical Analysis: Organic Compounds and Metal Complexes*; Verkade, J. B., Quin, L. D., Eds.; VCH: Weinheim, Germany, 1987.

(20) (a) Yamamoto, Y.; Yamazaki, H. *Bull. Chem. Soc. Jpn.* **1975**, *48*, 3691. (b) Treichel, P. M.; Wagner, K. P.; Hess, R. W. *Inorg. Chem.* **1973**, *12*, 1471.

(21) Michelin, R. A.; Bertani, R.; Mozzon, M.; Zanotto, L.; Benetollo, F.; Bombieri, G. *Organometallics* **1990**, *9*, 1449.

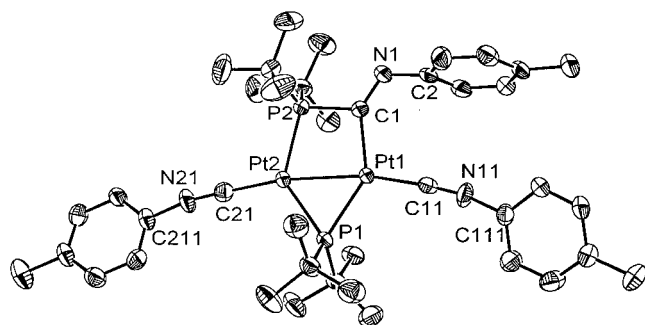


Figure 1. ORTEP view of the molecular structure of **8**. Thermal ellipsoids are drawn at 50% probability.

Table 2. Selected Bond Lengths (Å) and Angles (deg) for $[\text{Pt}_2(\mu\text{-P}(\text{Bu}'_2)\{\mu,\eta^2\text{-P}(\text{Bu}'_2)\text{C}(\text{=NAr})\}(\text{CNAr})_2)]$ (**8**) and $[\text{Pt}\{\mu,\eta^2\text{-P}(\text{Bu}'_2)\text{C}(\text{N}(\text{H})\text{Ar})\}(\text{CNAr})]_2(\text{CF}_3\text{SO}_3)_2$ (**11**)

	8	11
Pt1–Pt2	2.5980(3)	2.5838(6)
Pt1–P1	2.289(1)	2.303(3)
Pt2–P1	2.298(1)	
Pt2–P2	2.308(1)	2.301(3)
Pt1–C1	2.073(5)	2.04(1)
Pt2–C12		2.01(1)
Pt1–C11	1.911(6)	1.97(1)
Pt2–C21	1.923(6)	1.96(1)
P1–C12		1.84(1)
P2–C1	1.842(5)	1.84(1)
C11–N11	1.177(7)	1.16(2)
C21–N21	1.184(7)	1.17(2)
C1–N1	1.287(7)	1.32(2)
C12–N12		1.31(2)
N1–C2	1.412(7)	1.44(2)
N12–C22		1.43(1)
Pt2–Pt1–C11	168.3(1)	159.8(4)
Pt1–Pt2–C21	170.9(2)	164.3(5)
Pt1–C11–N11	174.5(5)	171.2(13)
Pt2–C21–N21	178.1(5)	175.3(12)
Pt1–P1–Pt2	69.01(4)	
P1–Pt1–C11	112.7(2)	103.4(4)
C1–Pt1–C11	106.9(2)	98.6(5)
P1–Pt2–C21	115.6(2)	
P1–Pt1–C1	140.4(1)	158.0(3)
P1–Pt2–P2	130.87(5)	
P2–Pt2–C12		157.4(3)
P2–Pt2–C21	113.5(2)	99.6(4)
C12–Pt2–C21		103.1(5)
Pt1–P1–C12		93.3(4)
Pt2–P2–C1	99.1(2)	93.5(4)
Pt1–C1–P2	100.5(2)	104.6(5)
Pt1–C1–N1	138.3(4)	130.2(9)
P2–C1–N1	120.9(4)	124.2(9)
Pt2–C12–P1		105.0(5)
Pt2–C12–N12		129.1(8)
P1–C12–N12		124.8(8)
C1–N1–C2	120.4(4)	123.8(11)
C12–N12–C22		123.5(10)
C11–N11–C111	168.5(6)	176.3(15)
C21–N21–C211	168.0(6)	176.5(15)
Pt1–P1–C12–Pt2		16.3(5)
Pt2–P2–C1–Pt1	0.1(2)	17.2(5)
P2–C1–N1–C2	177.9(4)	158(1)
P1–C12–N12–C22		164(1)

X-ray Structure of 8. An Ortep view of compound **8** is given in Figure 1, while selected bond lengths and angles are listed in Table 2. The structure consists of discrete Pt dimers held together by van der Waals forces. The immediate coordination sphere of the two metal atoms comprises a metal–metal bond (2.5980(3) Å), the two terminal *p*-tolyl isocyanide ligands, the intact bridging phosphido group and the “R₂P–CNR”

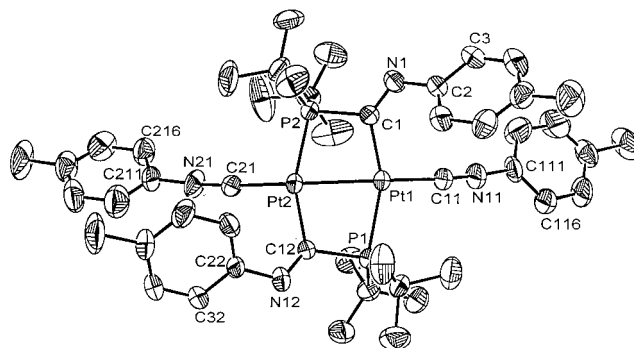


Figure 2. ORTEP view of the molecular structure of the cation **11**²⁺. Thermal ellipsoids are drawn at 50% probability.

moiety. The Pt–Pt separation falls in the expected range and is shorter but comparable to that found in the cation $[\text{Pt}_2(\mu\text{-P}(\text{Bu}'_2)(\text{H})(\text{PBu}'_2\text{H})_2)[\text{C}_3(\text{CN}_5)_5]$ (2.6473(5) Å),²² in keeping with the different electronic nature of the terminal ligands.

The two Pt–P1 distances are different (2.289(1) and 2.298(2) Å, respectively) as can be expected from the different trans influences exerted by P2 and C1. The C1–N1 and N1–C2 separations, at 1.287(7) and 1.412(7) Å, and the C1–N1–C2 angle (120.4(4)°) are consistent with the presence of a C=N–C moiety. All other distances are unexceptional.

The conformation of the isonitrile substituents can best be described by the dihedral angles between the least-squares planes through the *p*-tolyl rings and the coordination plane defined by atoms Pt1, Pt2, P1, and P2. We found, for the two terminal rings, angles of 19.9(2) and 18.6(3)°, respectively; the ring bond to atom N1 makes an angle of 79.9(1)° with the aforementioned plane.

X-ray Structure of 11. An Ortep view of the cation is given in Figure 2, while relevant geometric parameters are listed in Table 2. The most significant differences in the coordination geometry, compared to that of compound **8**, are (i) a small but significant shortening of the Pt–Pt separation (2.5838(6) vs 2.5980(3) Å), (ii) a lengthening of the terminal Pt–C distances (average values 1.965(7) and 1.917(8) Å, respectively), and (iii) a significant widening of the angles C11–N11–C111 (176.3(15) vs 168.5(6)°) and C21–N21–C211 (176.5(15) vs 168.0(6)°). These changes are consistent with the expected reduced back-donation of platinum in cation **11**²⁺.

As expected, the C1–N1 and C12–N12 bond lengths (average 1.315(7) Å) are longer than that found in **8** (1.287(7) Å), even though the lower precision of the structural determination of **11** prevents a detailed discussion of the changes induced by the protonation of the N atoms, as the differences in bonding parameters are marginally significant at the 3σ level; however, it may be noted that the H atoms bonded to N1 and N12 can be clearly located in the difference Fourier maps, thus confirming the proposed bonding scheme.

The steric crowding induced by the double insertion into the phosphido bridges is clearly reflected in the changes of the dihedral angles between the least-

(22) Leoni, P.; Pasquali, M.; Fortunelli, A.; Germano, G.; Albinati, A. *J. Am. Chem. Soc.* **1998**, *120*, 9564.

squares planes through the *p*-tolyl rings and the coordination plane defined by atoms Pt1, Pt2, P1, and P2. Thus, the dihedral angles between the coordination plane and the terminal rings are 41.7(5) and 36.7(6)°, respectively; those made by the bridging groups are 39.9(4) and 37.5(4)°, respectively.

Experimental Section

General Data. The reactions were carried out under a nitrogen atmosphere, by using standard Schlenk techniques. $[\text{Pt}_2(\mu\text{-P}^t\text{Bu}^t)_2(\text{P}^t\text{Bu}^t\text{H})(\text{CO})]$ (**1**) was prepared as previously described.¹³

Solvents were dried by conventional methods and distilled under nitrogen prior to use. IR spectra (Nujol mulls, KBr) were recorded on a Perkin-Elmer FT-IR 1725X spectrophotometer. NMR spectra were recorded on a Varian Gemini 200 BB instrument; frequencies are referenced to the residual resonances of the deuterated solvent (H, ¹³C), 85% H₃PO₄ (³¹P), and H₂PtCl₆ (¹⁹⁵Pt).

Preparation of $[\text{Pt}_2(\mu\text{-P}^t\text{Bu}^t)_2(\text{P}^t\text{Bu}^t\text{H})(\text{CN-}p\text{-tolyl})]$ (2**).** A toluene (0.2 mL) solution of *p*-tolyl isocyanide (0.109 mmol) was added by syringe to a yellow-orange toluene (15 mL) solution of complex **1** (91 mg, 0.106 mmol). The solution quickly turned deep orange, and after a few minutes, the solvent was evaporated and the residue suspended in acetonitrile (10 mL). An orange powder was isolated by filtration, washed with acetonitrile, and vacuum-dried (42 mg, 0.044 mmol, 42%). Anal. Calcd for C₃₂H₅₀N₂P₂Pt₂: C, 40.7; H, 6.62; N, 1.48. Found: C, 40.2; H, 6.53; N, 1.48. IR (Nujol, KBr): 2264 (ν_{PH}), 1936 (ν_{CN}) cm⁻¹. ¹H NMR (C₆D₆, 293 K): δ (ppm) 7.16 (m, 2H, Ar *H*), 6.71 (m, 2H, Ar *H*), 6.33 (dt, ¹J_{HP} = 324, ³J_{HP} = 15 Hz, with ¹⁹⁵Pt satellites, ²J_{HPt} = 17 Hz, P-*H*), 1.90 (s, 3H, *p*-CH₃), 1.55 (broad s, 36H, $\mu\text{-P}^t\text{Bu}^t$), 1.35 (d, ³J_{HP} = 14 Hz, 18H, PHBu^t). ¹³C{¹H} NMR (C₆D₆, 293 K): δ (ppm) 136.0 (s, C_{ipso}), 130.3 (s, CH [d, ¹J_{CH} = 160 Hz]), 129.9 (s, CH [d, ¹J_{CH} = 160 Hz]), 40.7 (s, PCCH₃), 34.7 (s, PCCH₃), 33.6 (m, PCCH₃ [quart, ¹J_{CH} = 125 Hz]), 31.5 (d, ²J_{CP} = 6.7 Hz, with satellites, ³J_{Cpt} = 23 Hz, PCCH₃ [quart, ¹J_{CH} = 120 Hz]), 21.1 (s, *p*-CH₃ [quart, ¹J_{CH} = 127 Hz]) (features from the proton-coupled spectrum are shown in brackets). See Table 1 for ³¹P and ¹⁹⁵Pt NMR parameters.

Complexes **3** and **4** were prepared by the same procedure, although they required longer (12 h) reaction times (yields 44 and 53%, respectively). The reactions were shown (³¹P NMR) to be nearly quantitative before isolation of the products. Complex **3**: Anal. Calcd for C₂₉H₅₅NP₃Pt₂: C, 37.7; H, 6.14; N, 2.06. Found: C, 37.3; H, 6.09; N, 2.02. IR (Nujol, KBr): 2259 (ν_{PH}), 1975 (ν_{CN}) cm⁻¹. ¹H NMR (C₆D₆, 293 K): δ (ppm) 6.34 (dt, ¹J_{HP} = 321, ³J_{HP} = 18 Hz, with satellites, ²J_{HPt} = 18 Hz, 1H, P-*H*), 1.57 (virtual triplet, ²³[³J_{HP} + ⁵J_{HP}] = 7 Hz, 36H, $\mu\text{-P}^t\text{Bu}^t$), 1.36 (d, ³J_{HP} = 14 Hz, 18H, PHBu^t), 1.22 (s, 9H, CN-*Bu*^t). ¹³C{¹H} NMR (C₆D₆, 293 K): δ (ppm) 40.9 (s, CCH₃), 40.4 (s, CCH₃), 40.1 (s, CCH₃), 33.6 (m, $\mu\text{-PCCH}_3$), 31.5 (d, ²J_{CP} = 7 Hz, with satellites, ³J_{Cpt} = 24 Hz, P(H)CCH₃) 31.2 (s, CN-CCH₃). See Table 1 for ³¹P and ¹⁹⁵Pt NMR parameters.

Complex **4**: Anal. Calcd for C₃₂H₆₀NP₃Pt₂: C, 40.8; H, 6.42; N, 1.49. Found: C, 40.3; H, 6.50; N, 1.47. IR (Nujol, KBr): 2256 (ν_{PH}), 2029 (ν_{CN}) cm⁻¹. ¹H NMR (C₆D₆, 293 K): δ (ppm) 7.3–7.0 (m, 5H, Ar *H*), 6.34 (dt, ¹J_{HP} = 317, ³J_{HP} = 17 Hz, with satellites, ²J_{HPt} = 18 Hz, 1H, P-*H*), 4.41 (s, with satellites, ⁴J_{HPt} = 8 Hz, 2 H, CNCH₂), 1.57 (virtual triplet, [³J_{HP} + ⁵J_{HP}] = 10 Hz, 36H, $\mu\text{-P}^t\text{Bu}^t$), 1.38 (d, ³J_{HP} = 14 Hz, 18H, PHBu^t). ¹³C{¹H} NMR (C₆D₆, 293 K): δ (ppm) 49.6 (s, CH₂), 40.7–28.0 (weak broad overlapping multiplets, CCH₃), 33.5 (m, $\mu\text{-PCCH}_3$), 31.5 (d, ²J_{CP} = 7 Hz, with broad satellites, P(H)CCH₃); the aromatic region is poorly resolved due to overlapping with the

resonances of the solvent (128 ppm). See Table 1 for ³¹P and ¹⁹⁵Pt NMR parameters.

Preparation of $[\text{Pt}_2(\mu\text{-P}^t\text{Bu}^t)_2(\text{CN-}p\text{-tolyl})_2]$ (5**).** A toluene (15 mL) solution of *p*-tolyl isocyanide (1.38 mmol) was added to a yellow-orange toluene (80 mL) solution of complex **1** (587 mg, 0.687 mmol). The solution quickly turned red, and after a few minutes, the solvent was evaporated and the residue suspended in acetonitrile (20 mL). An orange powder was isolated by filtration, washed with acetonitrile, and vacuum-dried (450 mg, 0.492 mmol, 72%). Anal. Calcd for C₃₂H₅₀N₂P₂Pt₂: C, 42.0; H, 5.51; N, 3.06. Found: C, 41.6; H, 5.63; N, 3.10. IR (Nujol, KBr): 2063, 2033 (broad, ν_{CN}) cm⁻¹. ¹H NMR (C₆D₆, 293 K): δ (ppm) 7.09 (d, ³J_{HH} = 8 Hz, 4H, Ar *H*), 6.68 (d, ³J_{HH} = 8 Hz, 4H, Ar *H*), 1.88 (s, 6H, *p*-CH₃), 1.61 (virtual triplet, [³J_{HP} + ⁵J_{HP}] = 7 Hz, 36H, $\mu\text{-P}^t\text{Bu}^t$). ¹³C{¹H} NMR (C₆D₆, 293 K): δ (ppm) 136.7, 129.8 (weak singlets, C_{ipso} and *p*-C), 130.3, 124.4 (s, *o*-C and *m*-C), 40.9 (m, PCCH₃), 32.7 (m, PCCH₃), 20.8 (s, *p*-CH₃). See Results and Discussion for ³¹P and ¹⁹⁵Pt NMR parameters.

Complexes **6** and **7** were prepared by the same procedure, although they required longer reaction times (12 h at 20 °C and 72 h at 30 °C, respectively) and higher excess of the corresponding isonitrile (yield 54 and 48%, respectively). The reactions were shown (³¹P NMR) to be nearly quantitative before isolation of the products.

Complex **6**: Anal. Calcd for C₂₆H₅₄N₂P₂Pt₂: C, 36.9; H, 6.43; N, 3.31. Found: C, 37.2; H, 6.39; N, 3.32. IR (Nujol, KBr): 2175, 2167 (broad, ν_{CN}) cm⁻¹. ¹H NMR (toluene-*d*₈, 293 K): δ (ppm) 1.74 (virtual triplet, [³J_{HP} + ⁵J_{HP}] = 6 Hz, 36H, $\mu\text{-P}^t\text{Bu}^t$), 1.46 (s, 18H, CN*Bu*^t). ¹³C{¹H} NMR (C₆D₆, 293 K): δ (ppm) 40.3 (weak broad overlapping multiplets, CCH₃), 33.2 (broad s, PCCH₃), 31.0 (broad s, CN-CCH₃). See Results and Discussion for ³¹P and ¹⁹⁵Pt NMR parameters.

Complex **7**: Anal. Calcd for C₃₂H₅₀N₂P₂Pt₂: C, 42.0; H, 5.51; N, 3.06. Found: C, 42.2; H, 5.49; N, 3.04. IR (Nujol, KBr): 2073 (broad, ν_{CN}) cm⁻¹. ¹H NMR (C₆D₆, 293 K): δ (ppm) 7.4–6.7 (m, 10H, Ar *H*), 4.31 (s, with satellites, ⁴J_{HPt} = 9 Hz, 4H, CH₂), 1.58 (virtual triplet, [³J_{HP} + ⁵J_{HP}] = 7 Hz, 36H, $\mu\text{-P}^t\text{Bu}^t$). ¹³C{¹H} NMR (C₆D₆, 293 K): δ (ppm) 48.9 (s, CH₂), 40.2 (s, PCCH₃), 32.9 (br s, PCCH₃); the aromatic region is poorly resolved due to overlapping with the resonances of the solvent (128 ppm). See Results and Discussion for ³¹P and ¹⁹⁵Pt NMR parameters.

Preparation of $[\text{Pt}_2(\mu\text{-P}^t\text{Bu}^t)\{\mu,\eta^2\text{-P}(\text{Bu}^t)_2\text{C}(\text{=N-}p\text{-tolyl})\}(\text{CN-}p\text{-tolyl})_2]$ (8**).** A toluene (1.5 mL) solution of *p*-tolyl isocyanide (0.787 mmol) was added to a yellow-orange toluene (20 mL) solution of complex **1** (192 mg, 0.225 mmol). The solution quickly turned deep orange and slowly (1 h) deep red, the solvent was evaporated, and the residue suspended in *n*-hexane (15 mL). A green-brown crystalline solid was isolated by filtration and vacuum-dried (107 mg, 0.102 mmol, 46%). Anal. Calcd for C₄₀H₅₇N₃P₂Pt₂: C, 46.5; H, 5.57; N, 4.07. Found: C, 46.1; H, 5.53; N, 4.03. IR (Nujol, KBr): 2073, 2040 (broad, ν_{CN}), 1537 ($\nu_{\text{C=N}}$) cm⁻¹. ¹H NMR (CD₂Cl₂, 293 K): δ (ppm) 7.30 (m, 4H, Ar *H*), 7.12 (d, ²J_{HH} = 8 Hz, 2H, Ar *H*), 7.01 (d, ²J_{HH} = 8 Hz, 2H, Ar *H*), 6.83 (m, 4H, Ar *H*), 2.40 (s, 3H, *p*-CH₃), 2.31 (s, 3H, *p*-CH₃), 2.10 (s, 3H, *p*-CH₃), 1.41 (d, ³J_{HP} = 13 Hz, 18H, PCCH₃), 1.34 (d, ³J_{HP} = 15 Hz, 18H, PCCH₃). ¹³C{¹H} NMR (CDCl₃, 293 K): δ (ppm) 130.5 (s, CH, [d, 159 Hz]), 129.8 (s, CH, [d, 164 Hz]), 128.9 (s, CH, [d, 154 Hz]), 125.2 (s, CH, [d, 167 Hz]), 125.0 (s, CH, [d, 167 Hz]), 121.0 (s, CH, [d, 169 Hz]), 40.0 (s, PCCH₃), 38.4 (s, PCCH₃), 33.3 (m, PCCH₃, [q, 126 Hz]), 29.5 (m, PCCH₃, [q, 127 Hz]), 21.7 (2 overlapping singlets, *p*-CH₃, [q, 130 Hz]), 21.1 (s, *p*-CH₃, [q, 129 Hz]) (features from the proton-coupled spectrum are shown in brackets). See Results and Discussion for ³¹P and ¹⁹⁵Pt NMR parameters. The reaction was shown (³¹P NMR) to be nearly quantitative before isolation of the product.

Preparation of $[\text{Pt}\{\mu,\eta^2\text{-P}(\text{Bu}^t)_2\text{C}(\text{=N-}p\text{-tolyl})\}(\text{CN-}p\text{-tolyl})_2]$ (9**).** A toluene (2.5 mL) solution of *p*-tolyl isocyanide (1.28 mmol) was added to a yellow-orange toluene (40 mL)

solution of complex **1** (219 mg, 0.256 mmol). The solution quickly turned deep orange and slowly (1 h) deep red, the solvent was evaporated, and the residue was suspended in *n*-hexane (10 mL). A deep green powder was isolated by filtration and vacuum-dried (170 mg, 0.147 mmol, 57%). Anal. Calcd for $C_{48}H_{64}N_4P_2Pt_2$: C, 50.2; H, 5.61; N, 4.88. Found: C, 50.5; H, 5.58; N, 4.83. IR (Nujol, KBr): 2107 (broad, ν_{CN}), 1542 ($\nu_{C=N}$) cm^{-1} . 1H NMR (C_6D_6 , 293 K): δ (ppm) 7.60 (m, 4H, Ar H), 7.10 (m, 4H, Ar H), 6.64 (m, 8H, Ar H), 2.02 (s, 6H, $p-CH_3$), 1.84 (s, 6H, $p-CH_3$), 1.65 (m, 36H, $PCCCH_3$). $^{13}C\{^1H\}$ NMR (C_6D_6 , 293 K): δ (ppm) 129.4 (s, CH), 128.0 (s, CH), 124.9 (s, CH), 121.2 (s, CH), 36.9 (s, $PCCCH_3$), 29.7 (s, $PCCH_3$), 20.7 (br s, $p-CH_3$). See Results and Discussion for ^{31}P and ^{195}Pt NMR parameters. The reaction was shown (^{31}P NMR) to be nearly quantitative before isolation of the product.

Preparation of $[Pt_2(\mu-PBu'_2)\{\mu,\eta^2-P(Bu'_2)C(NHAr)\}(CNAr)_2]CF_3SO_3$ (10**).** A red toluene (15 mL) solution of complex **8** (139 mg, 0.135 mmol) quickly turned brown after the addition of CF_3SO_3H (12 μL , 0.136 mmol), and a red solid started to precipitate out. The suspension was stirred for 1 h at ambient temperature, and the solid was isolated by filtration, washed with *n*-hexane, and vacuum-dried (86 mg, 55% yield). Anal. Calcd for $C_{41}H_{58}F_3N_3O_3P_2Pt_2S$: C, 38.6; H, 4.90; N, 3.37. Found: C, 39.1; H, 4.93; N, 3.35. 1H NMR ($CDCl_3$, 293 K): δ (ppm) 14.3 (br s, with ^{195}Pt satellites, $^3J_{HPt} = 120$ Hz, 1 H, NH), 8.0 (d, $J_{HH} = 7.8$ Hz, 2 H, Ar H), 6.9 (m, 4 H, Ar H), 6.7 (d, $J_{HH} = 8.1$ Hz, 2 H, Ar H), 6.6 (d, $J_{HH} = 8.3$ Hz, 2 H, Ar H), 6.5 (d, $J_{HH} = 8.3$ Hz, 2 H, Ar H), 1.95 (s, 3 H, CH_3), 1.9 (s, 3 H, CH_3), 1.8 (s, 3 H, CH_3), 1.4 (m, 36 H, CH_3). $^{13}C\{^1H\}$ NMR ($CDCl_3$, 293 K): δ (ppm) 139.8 s [s], 139.5 s [s], 122.9 s [s], 131.2 s [d, $^1J_{CH} = 163$ Hz], 130.8 s [d, $^1J_{CH} = 163$ Hz], 130.3 s [d, $^1J_{CH} = 172$ Hz], 129.3 s [d, $^1J_{CH} = 160$ Hz], 126.9 s [d, $^1J_{CH} = 164$ Hz], 125.7 s [d, $^1J_{CH} = 164$ Hz], 40.8 s [s], 39.3 s [s], 33.0 s [q, $^1J_{CH} = 134$ Hz], 30.1 s [q, $^1J_{CH} = 135$ Hz], 21.6 (3 overlapping s) [q, $^1J_{CH} = 128$ Hz] (features from the proton-coupled spectrum are shown in brackets). See Results and Discussion for ^{31}P and ^{195}Pt NMR spectra. IR (Nujol, KBr): 2105 (ν_{CN}), 1263, 1153, 1030, 637 (uncoordinated triflate) $^{24} cm^{-1}$.

Preparation of $[Pt\{\mu,\eta^2-P(Bu'_2)C(NHAr)\}(CNAr)_2](CF_3SO_3)_2$ (11**).** A red toluene (10 mL) solution of complex **9** (70 mg, 0.061 mmol) quickly turned brown after the addition of CF_3SO_3H (12 μL , 0.136 mmol), and an orange solid started to precipitate out. The suspension was stirred for 1 h at ambient temperature, and the solid was filtered, washed with Et_2O , and vacuum-dried (52 mg, 57%). Anal. Calcd for $C_{50}H_{66}F_6N_4O_6P_2Pt_2S_2$: C, 41.4; H, 4.59; N, 3.87. Found: C, 41.2; H, 4.59; N, 3.91. $^{31}P\{^1H\}$ NMR ($CDCl_3$, 293 K): δ (ppm) 37.8 (s, with ^{195}Pt satellites, $^2J_{PP} = 90$, $^1J_{PPt} = 1820$, $^2J_{PPt} = -260$ Hz from simulated spectra). 1H NMR ($CDCl_3$, 293 K): δ (ppm) 13.5 (br t, $J \approx 15$ Hz, with broad ^{195}Pt satellites, $^3J_{HPt} = 128$ Hz, 2 H, NH), 7.8 (d, $J_{HH} = 8.2$ Hz, 4 H, Ar H), 7.2 (d, $J_{HH} = 8.2$ Hz, 8 H, Ar H), 6.8 (d, $J_{HH} = 8.2$ Hz, 4 H, Ar H), 2.4 (s, 6 H, CH_3), 2.2 (s, 6 H, CH_3), 1.5 (d, $^3J_{HP} = 15$ Hz, 36 H, CH_3). $^{13}C\{^1H\}$ NMR ($CDCl_3$, 293 K): δ (ppm) 130.3 s [d, $^1J_{CH} = 160$ Hz], 129.0 s [d, $^1J_{CH} = 161$ Hz], 125.5 s [d, $^1J_{CH} = 163$ Hz], 124.2 s [d, $^1J_{CH} = 163$ Hz], 141.3 s [s], 38.0 s [s], 30.5 s [q, $^1J_{CH} = 148$ Hz], 21.5 (2 overlapping s) [q, $^1J_{CH} = 129$ Hz] (features from the proton-coupled spectrum are shown in brackets). $^{195}Pt\{^1H\}$ NMR ($CDCl_3$, 293 K): δ (ppm) -4496 (dd, $^1J_{PtP} = 1820$, $^2J_{PtP} = -260$ Hz) [$^3J_{PtH} = 128$ Hz from the proton-coupled spectrum]. IR (Nujol, KBr): 2147 (ν_{CN}), 1262, 1156, 1033, 637 (uncoordinated triflate) cm^{-1} .

Crystallography. Air-stable crystals of $[Pt_2(\mu-PBu'_2)\{\mu,\eta^2-P(Bu'_2)C(=NAr)\}(CNAr)_2]$ (**8**) were obtained by recrystallization from toluene-hexane mixtures.

Crystals of $[Pt\{\mu,\eta^2-P(Bu'_2)C(NHAr)\}(CNAr)_2](CF_3SO_3)_2$ (**11**), suitable for X-ray diffraction, were obtained by crystallization from CH_2Cl_2/Et_2O and are air stable.

Table 3. Experimental Data for the X-ray Diffraction Study of Compounds: $[Pt_2(\mu-PBu'_2)\{\mu,\eta^2-P(Bu'_2)C(=NAr)\}(CNAr)_2]$ (8**) and $[Pt\{\mu,\eta^2-P(Bu'_2)C(NHAr)\}(CNAr)_2](CF_3SO_3)_2$ (**11**)**

	8	11
formula	$C_{40}H_{57}N_3P_2Pt_2$	$C_{50}H_{66}F_6N_4O_6P_2Pt_2S_2$
mol wt	1032.03	1449.31
data coll. T, K	200(2)	293(2)
radiation	Mo K α (graphite monochromated, $\lambda = 0.710\ 69\ \text{\AA}$)	
cryst syst	triclinic	monoclinic
space group	$P\bar{1}$ (No. 2)	$P2_1/n$ (No. 14)
a, \AA	11.1702(1)	13.0470(6)
b, \AA	11.1723(1)	10.4100(5)
c, \AA	18.6149(2)	43.706 (2)
α , deg	95.965(1)	90.0
β , deg	107.333(1)	90.43(1)
γ , deg	108.290(1)	90.0
V, \AA^3	2062.77(3)	5935.9(5)
Z	2	4
$\rho(\text{calcd})$, $g\ cm^{-3}$	1.662	1.621
μ , mm^{-1}	6.881	4.898
θ range, deg	$1.17 < \theta < 25.66$	$1.63 < \theta < 29.45$
transmissn factors	0.291–0.180	1.000–0.732
no. of indep rflns, n_0	6855	15105
no. of obsd rflns	5805	12615
($ F_o > 4.0\sigma(F)$)		
no. of params, n_v	424	621 (3)
(no. of restraints)		
R1, obsd rflns	0.0258 (0.0351)	0.0763 (0.0924)
(all data) ^a		
wR2, obsd rflns	0.0583 (0.0629)	0.1204 (0.1312)
(all data) ^b		
GOF ^c	1.088	0.784

^a $R = \sum(|F_o - (1/k)F_c|)/\sum|F_o|$. ^b $wR2 = [\sum w(F_o^2 - (1/k)F_c^2)^2]/\sum w|F_o^2|^2$. ^c $GOF = [\sum w(F_o^2 - (1/k)F_c^2)^2/(n_0 - n_v)]^{1/2}$.

Prismatic single crystals of both compounds were mounted, for the data collection, on a glass fiber at a random orientation, on a Bruker SMART CCD diffractometer at 200 K for **8** and at room temperature for **11**.

The space groups were unambiguously determined from the systematic absences, while the cell constants were refined at the end of the data collection with the data reduction software SAINT.²⁵ Data were collected by using ω scans in steps of 0.3° ; for compound **8** 2142 frames were collected with a counting time of 20 s, while for **11** 2450 frames were measured, each being counted for 20 s. A list experimental conditions for the data collection is given in Table S1 in the Supporting Information.

The measured intensities were corrected for Lorentz and polarization factors²⁵ and empirically for absorption using the SADABS program.²⁶

Selected crystallographic and other relevant data are listed in Table 3 and in Table S1.

The standard deviations on intensities were calculated in term of statistics alone, while those on F_o^2 were calculated as shown in Table S1.

All calculations were carried out by using the PC version of the SHELX-97 programs.²⁷ The scattering factors used, corrected for the real and imaginary parts of the anomalous dispersion, were taken from the literature.²⁸

Structural Study of $[Pt_2(\mu-PBu'_2)\{\mu,\eta^2-P(Bu'_2)C(=NAr)\}(CNAr)_2]$ (8**).** The structure was solved by direct and Patterson methods.

(25) SAINT: SAX Area Detector Integration: Siemens Analytical Instrumentation, 1996.

(26) Sheldrick, G. M. SADABS, Universität Göttingen, Göttingen, Germany (to be submitted for publication).

(27) Sheldrick, G. M. SHELX-97: Structure Solution and Refinement Package; Universität Göttingen, Göttingen, Germany, 1997.

(28) *International Tables for X-ray Crystallography*; Wilson, A. J. C. Ed.; Kluwer Academic: Dordrecht, The Netherlands, 1992; Vol. C.

Data were refined by full-matrix least squares,²⁷ minimizing the function $\sum w(F_o^2 - (1/k)F_c^2)^2$. Anisotropic displacement parameters were used for all atoms, while the contribution of the hydrogen atoms, in their calculated positions ($C-H = 0.95$ Å, $B(H) = 1.5[B(C_{\text{bonded}})]$ Å²), was included in the refinement using a riding model.

No extinction correction was deemed necessary. Upon convergence (see Table S1) the final Fourier difference map showed no significant peaks.

Structural Study of $[\text{Pt}\{\mu, \eta^2\text{-P}(\text{Bu}^t_2)\text{C}(\text{NAr})\}(\text{CNAr})]_2(\text{CF}_3\text{SO}_3)_2$ (11**).** The structure was solved and refined as above using anisotropic displacement parameters for all atoms. The contribution of the hydrogen atoms, in their calculated positions ($C-H = 0.95$ Å, $B(H) = 1.5[B(C_{\text{bonded}})]$ Å²), was included in the refinement using a riding model. No extinction correction was deemed necessary.

As can be seen from the large values of their atomic displacements, the triflate counterions are disordered and their unconstrained refinement led to unacceptable geometries. Therefore, a model was constructed using the strongest peaks of a difference Fourier map and constrained to retain a tetrahedral geometry (around the carbon and sulfur atoms) but allowing the C-F and S-O distances to vary.

Upon convergence (see Table S1) the final Fourier difference map showed no significant peaks.

Acknowledgment. The Consiglio Nazionale delle Ricerche (CNR) and MURST, Programmi di Interesse Nazionale, 1998-9, are gratefully acknowledged for financial support. A.A. and F.E. wish to thank the Vigoni program for partial support.

Supporting Information Available: Text giving experimental details and a full listing of crystallographic data for compounds **8** and **11**, including tables of positional and isotropic equivalent displacement parameters, calculated positions of the hydrogen atoms, anisotropic displacement parameters, bond distances and angles, and ORTEP figures showing the full numbering schemes, and experimental and calculated ³¹P{¹H} and ¹⁹⁵Pt{¹H} NMR spectra of complex **9**. This material is available free of charge via the Internet at <http://pubs.acs.org>.

OM000461T